

Spin-singlet state formation in the cluster Mott insulator GaNb_4S_8 studied by μSR and NMR spectroscopy

T. Waki, Y. Kajinami, Y. Tabata, and H. Nakamura

Department of Materials Science and Engineering, Kyoto University, Kyoto 606-8501, Japan

M. Yoshida and M. Takigawa

Institute for Solid State Physics, University of Tokyo, Kashiwa 277-8581, Japan

I. Watanabe

Advanced Meson Science Laboratory, RIKEN Nishina Center, Wako 351-0198, Japan

(Received 1 November 2009; published 6 January 2010)

Muon spin relaxation (μSR) and nuclear magnetic resonance experiments revealed that the spin-singlet state with an excitation gap of ~ 200 K is realized from $S=1/2$ Nb_4 tetrahedral clusters in a cluster Mott insulator GaNb_4S_8 . The intercluster cooperative phenomenon to the singlet state at $T_S=32$ K is triggered by intracuster Jahn-Teller type structural instability developed from $\sim 3T_S$. Referring to the lattice symmetry, the formation of Nb_8 octamer (Nb_4 - Nb_4 bond) is suggested.

DOI: [10.1103/PhysRevB.81.020401](https://doi.org/10.1103/PhysRevB.81.020401)

PACS number(s): 75.30.Kz, 75.50.-y, 76.75.+i, 76.60.-k

In any magnets, if spin is well defined at the atomic site, the classical spin degree of freedom must be compensated on approaching 0 K, which is usually achieved by magnetic order. Another route via electron-lattice coupling is quenching of spin itself by formation of a spin-singlet state. It is of interest to extend this concept to cluster compounds with mixed-valent magnetic clusters (more than one atom shares unpaired electrons within the cluster unit) embedded in a matrix crystal. When the cluster unit has half-integer spin, particularly, since intracuster interactions never compensate all the spin, we expect long-range magnetic order due to minor intercluster interactions. In this Rapid Communications, we show another possibility, formation of a bound state between clusters, such as dimerization in the one-dimensional (1D) $S=1/2$ spin chain with the electron-lattice coupling.¹

As a category of mixed-valent magnetic cluster compounds, ternary calcogenides AB_4X_8 ($A=\text{Ga, Al, Ge}$; $B=\text{V, Mo, Nb, Ta}$; $X=\text{S, Se}$) with the cubic GaMo_4S_8 structure (space group $F\bar{4}3m$)²⁻⁴ are of particular interest. In the compounds, cubic $(B_4X_4)^{n+}$ and tetrahedral $(AX_4)^{n-}$ ions are weakly coupled in a NaCl manner, resulting in hopping conduction between the clusters. GaNb_4S_8 with $(\text{Nb}_4\text{S}_4)^{5+}$ and $(\text{GaS}_4)^{5-}$ ions has attracted attention as a sort of Mott insulator, where $4d$ electrons are localized at Nb_4 clusters due to electron correlations, and also as one of pressure-induced superconductors.⁵ In molecular orbital schemes, the tetrahedral Nb_4 unit in $(\text{Nb}_4\text{S}_4)^{5+}$ shares seven $4d$ electrons, resulting in one unpaired electron at the highest occupied molecular orbital (HOMO) as shown in Fig. 1.⁵ In other words, the Nb_4 tetramer has a local moment with $S=1/2$. Accordingly, the magnetic susceptibility χ obeys the Curie-Weiss law with the effective moment $\mu_{\text{eff}}=1.73 \mu_B/\text{f.u.}$ ⁵ The negative Weiss constant $\theta=-298$ K suggests antiferromagnetic (AF) coupling among clusters. χ shows an abrupt drop at $T_S=32$ K, which is accompanied by a structural transition to a tetragonal state ($P\bar{4}2_1m$) (Ref. 6) possibly due to Jahn-Teller (JT) type instability; the triply degenerate HOMO splits to singlet

and doublet states (see Fig. 1). Concerning the magnetic ground state below T_S , Pocha *et al.*⁵ commented no additional reflections in powder neutron diffraction profiles, ruled out long-range AF order, and then ascribed the absence of long-range order to topological spin frustration. On the other hand, in a more recent paper, Jacob *et al.*⁶ proposed noncollinear AF order on the basis of their crystallographic analysis and band structure calculations. Being inconsistent with $S=1/2$ inherent to the cluster, our muon spin relaxation (μSR) and nuclear magnetic resonance (NMR) experiments clearly indicate presence of a spin excitation gap below T_S , namely, compensation of spin to the $S=0$ state. Referring to the lattice symmetry,⁵ we discuss possible Nb_8 octamer formation from two Nb_4 tetramers.

All polycrystalline samples were prepared by solid state reaction from pure elements sealed in evacuated quartz tubes. Final heat treatment was performed at 900 °C for 1 day after several heat treatments and intermediate regrinds. χ , measured to check sample quality using a commercial SQUID magnetometer (Quantum Design, MPMS) equipped in LTM, Kyoto University, was the same as literature data^{3,5,6} (our result is shown in Fig. 3). Zero-field (ZF) and longitudinal-field (LF) μSR measurements were made at the RIKEN-RAL Muon Facility at the Rutherford-Appleton Laboratory in the U.K. using a pulsed positive surface muon beam at 4.5–100 K under LF fields of 0–0.4 T. NMR experiments for ^{69,71}Ga (nuclear spin $I=3/2$ for both) and ⁹³Nb

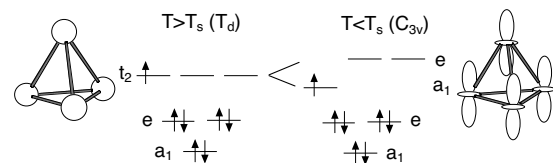


FIG. 1. Proposed molecular orbital schemes of the Nb_4 unit above and below T_S .⁵ To interpret isotropic and anisotropic hyperfine fields at the Nb site, schematic spin density distributions are shown for HOMO.

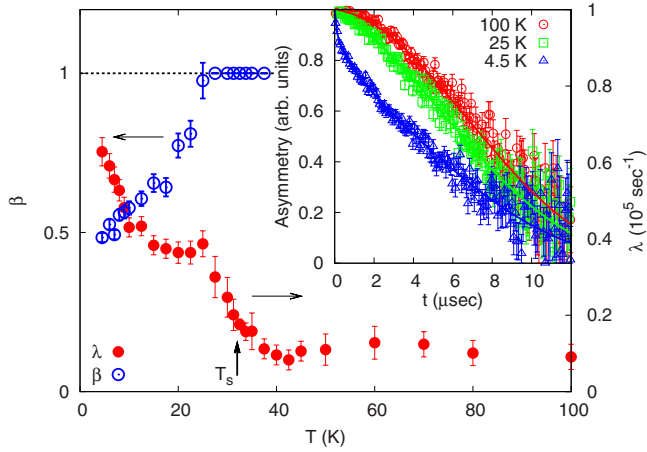


FIG. 2. (Color online) The T dependence of the ZF muon spin relaxation rate λ . The inset shows typical examples of ZF- μ SR spectra (at 4.5, 25, and 100 K). Solid curves indicate the fit by the damped KT function. Below T_S , the asymmetry is fit with the stretched exponential function.

($I=9/2$) were performed with a standard phase coherent spectrometer. Most NMR spectra were obtained by Fourier transform of the spin-echo or free-induction decay signal in a fixed magnetic field of 7.0071 T. The nuclear spin-lattice relaxation rate $1/T_1$ for $^{69,71}\text{Ga}$ was obtained by inversion and saturation recovery methods. ^{93}Nb - T_1 is too short to be estimated reliably.

To determine the magnetic ground state, we first show results of μ SR. Since NMR is affected by both magnetic and electric hyperfine interactions, the analysis of powder-pattern spectra is often nonstraightforward. In contrast, μ SR probes only the magnetic field, and has an advantage in monitoring the appearance of internal fields. Typical examples of ZF- μ SR spectra are shown in the inset of Fig. 2. Even at the lowest temperature (T), no evidence of magnetic order such as muon spin precession was observed. Above T_S , the relaxation is dominated by Gaussian-like depolarization. The commonly used damped Kubo-Toyabe (KT) function $P_\mu(t) = \exp(-\lambda t) G_z^{\text{KT}}(\Delta, t)$ with $G_z^{\text{KT}}(\Delta, t) = \frac{1}{3} + \frac{2}{3}(1 - \Delta^2 t^2) \exp(-\frac{1}{2} \Delta^2 t^2)$ was fit to the data, where Δ/γ_μ is the width of the static field distribution (γ_μ : muon gyromagnetic ratio), and λ is the damping rate associated with an additional relaxation process mostly due to electron spin fluctuations. Above T_S , by treating λ and Δ as free fitting parameters, we obtained a nearly T -independent value of $\Delta \approx 0.1 \times 10^6 \text{ s}^{-1}$, which corresponds to a tiny field of $\Delta/\gamma_\mu \approx 1 \text{ G}$, and is ascribed to dipolar fields coming from randomly oriented nuclear spins. With decreasing T passing through T_S , due to an appearance of fast relaxation, the above function tunes to be inappropriate. We phenomenologically applied the stretched exponential function $P_\mu(t) = \exp[-(\lambda t)^\beta] G_z^{\text{KT}}(\Delta, t)$ to fit low- T data, where β is a free parameter. β depends on T and gradually deviates from 1 and reaches to 0.5 at lowest T suggesting gradual development of distribution of relaxation. In addition, associated with appearance of the fast relaxation, the damping part (dynamic fields) tends to mask the Gaussian part (small static fields), resulting in unreliable estimation of Δ below $\sim 30 \text{ K}$. Then

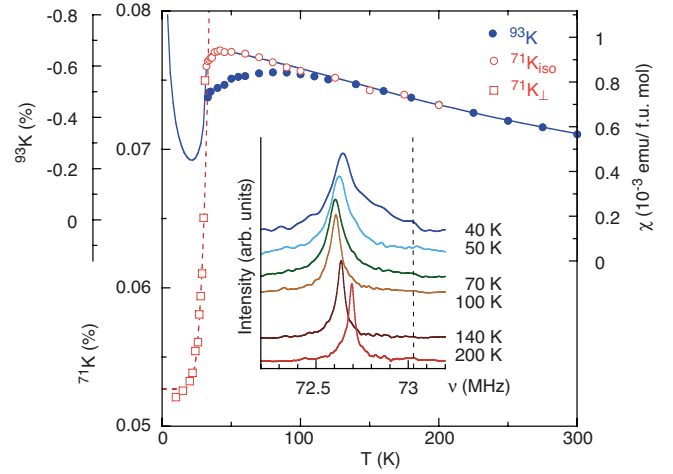


FIG. 3. (Color online) T dependences of ^{93}Nb and ^{71}Ga hyperfine shifts, ^{93}K above T_S (solid circles), $^{71}\text{K}_{\text{iso}}$ above T_S (open circles) and $^{71}\text{K}_\perp$ below T_S (open squares) (Ref. 10). The solid curve indicates the bulk susceptibility χ . The broken curve represents $\exp(-E_g/k_B T)$ with $E_g/k_B \approx 220 \text{ K}$. The inset shows ^{93}Nb -NMR lines (only the center line) above T_S , measured under an external field of 7.0071 T. The broken straight line indicates the zero shift position.

we assumed T independence of Δ , only for simplicity, to analyze low- T data. Thus, estimated λ is increased below T_S whereas the cusp of λ at around 22 K may be an artifact due to fitting. The enhancement of λ is often seen for the system, which condenses into a spin singlet state,⁷ although the origin is still under debate. In LF- μ SR experiments below T_S , strong muon-spin depolarization was observed in the whole range of LF up to 0.4 T. This observation indicates the presence of dynamic components of electronic spins and supports the absence of large static field due to static magnetic order. Hence, we conclude that the ground state is neither long-range nor short-range magnetic order.

Next, let us see NMR data. Examples of ^{93}Nb -NMR lines measured above T_S are shown in the inset of Fig. 3, where only the center line (the $m = -1/2 \leftrightarrow 1/2$ transition) is shown. Nearby the sharp center line, unresolved satellites due to quadrupole interaction, spreading out in several hundred kHz, were observed; the Nb atom occupies an axially symmetric site (16e) in the high- T cubic state. With decreasing T , the resonance frequency once decreases until $\sim 80 \text{ K}$ and increases again. The T dependence of the magnetic hyperfine shift ^{93}K , estimated from the peak position, is shown in Fig. 3. A high- T part of ^{93}K scales well with χ .⁸ $|^{93}\text{K}|$ exhibits a characteristic broad hump at $\sim 80 \text{ K}$, deviating from a Curie-Weiss-like T dependence at high T .⁹ Furthermore, note that the lineshape turns to be strongly asymmetric in spite of the reduction of $|^{93}\text{K}|$. The origin of the characteristic hump and anisotropy of ^{93}K will be discussed later. Below T_S , the ^{93}Nb spectrum turns to be broad and complex. This is mainly due to separation of the Nb site to three crystallographically inequivalent sites (8f and two 4e) and appearance of large anisotropy in ^{93}K . Here, we do not discuss further the low- T ^{93}Nb spectrum, because the analysis is not straightforward but complicated.

Figure 4(a) shows ^{71}Ga -NMR lines above T_S . A single

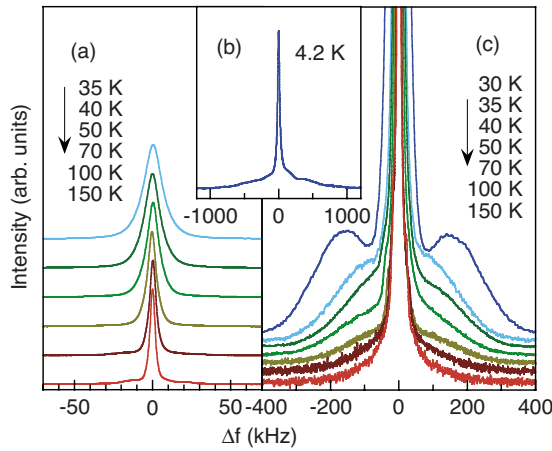


FIG. 4. (Color online) ^{71}Ga spectra measured above T_S (a) and below T_S (b), and magnified bottom structures above T_S (c). The data were collected in a field of 7.0071 T and plotted with respect to peak positions. The spectrum of (b) was obtained by summing Fourier transforms of the spin-echo signal accumulated at different frequencies.

symmetric line accords with the cubic symmetry of the Ga site (4a) above T_S . With decreasing T , the line is broadened. We confirmed that the linewidth is magnetic in origin; the ratio of ^{69}Ga and ^{71}Ga linewidths is T independent and close to $^{69}\gamma/^{71}\gamma=0.7870$ (γ : gyromagnetic ratio) but different from $^{69}Q/^{71}Q=1.60$ (Q : quadrupole moment). The ^{71}Ga hyperfine shift, ^{71}K , estimated from the peak position, is also plotted in Fig. 3.¹⁰ ^{71}K is in reasonable proportion to χ at least above T_S (Ref. 8) in contrast to the case of ^{93}K . Below T_S , ^{71}K drops suddenly, and approaches a constant value at low T , proving that the low- T upturn in χ is extrinsic. In addition, another component extended over 2 MHz appears on the foot of the center line as shown in Fig. 4(b). This bottom component is most reasonably assigned to quadrupole satellites. According to the lattice symmetry,⁶ a single Ga site (nonaxial 2c) exists only even below T_S . The unresolved satellites are reasonable if considerable asymmetry appears in ^{71}K ; the center line looks asymmetric. Focusing on the bottom part, the T variation is shown in Fig. 4(c). Note that the quadrupole broadening already appears well above T_S in spite of the nominal cubic symmetry at the Ga site in the high T state. The result indicates that local environments around the Ga site already gets distorted well above T_S .

Figure 5(a) shows T dependences of $1/T_1$ for $^{69,71}\text{Ga}$. The recovery of nuclear magnetization fits well with a single exponential function well above T_S , with two exponential functions expected for the $I=3/2$ nucleus with quadrupole interaction just above T_S , and with neither the single exponential nor the $I=3/2$ function below T_S . These facts are, as a whole, consistent with the observation in the static spectrum. The last fact indicates the distribution of $1/T_1$, which is attributable to the appearance of hyperfine anisotropy. Below T_S , $1/T_1$ was estimated by applying tentatively a stretched exponential function $\exp[-(t/T_1)^\beta]$ (obtained β is nearly T independent of ~ 0.6). With decreasing T , $^{71}(1/T_1)$ once decreases to reach a minimum at ~ 50 K, increases again to

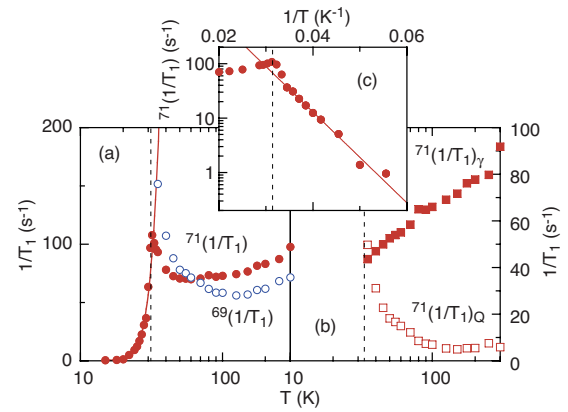


FIG. 5. (Color online) (a) T dependences of $1/T_1$ measured for ^{69}Ga (open circles) and ^{71}Ga (closed circles). Reliable $^{69}(1/T_1)$ was not obtained below T_S due to overlap of ^{93}Nb and ^{69}Ga signals. (b) T dependences of quadrupole (open squares) and magnetic (solid squares) components of $^{71}(1/T_1)$. (c) The Arrhenius plot of $^{71}(1/T_1)$ at low T . The solid line, corresponding to the solid curve in (a), gives $E_g/k_B \approx 190$ K.

take a sharp peak at T_S and drops abruptly below T_S .

Measurements of $1/T_1$ for different isotopes $^{69,71}\text{Ga}$ give valuable information on spin and lattice dynamics. As seen in Fig. 5(a), magnitudes of $^{69}(1/T_1)$ and $^{71}(1/T_1)$ are reversed at ~ 60 K. Because of $^{69}\gamma/^{71}\gamma < 1$ and $^{69}Q/^{71}Q > 1$, this implies that both magnetic and electric quadrupole fluctuations contribute to $1/T_1$, and furthermore depend differently on T . $1/T_1$ for the nucleus with I and Q is expressed as the superposition of magnetic and quadrupole terms, $1/T_1 = (1/T_1)_\gamma + (1/T_1)_Q$. Figure 5(b) shows T dependences of separated contributions, estimated by solving simultaneous equations for $^{69}(1/T_1)$ and $^{71}(1/T_1)$ with use of relations $(1/T_1)_\gamma \propto \gamma^2$ and $(1/T_1)_Q \propto Q^2$. The magnetic component decreases monotonically, indicating no enhancement toward T_S . For the system with dynamically fluctuating local moments, we expect T -independent $1/T_1$. The gradual decrease of $1/T_1$ is possibly ascribed to the development of spin-singlet correlations. On the other hand, interestingly, the quadrupole contribution shows a critical behavior on approaching T_S . This enhancement indicates that structural fluctuations develop from ~ 100 K, of the order of $3T_S$. The fluctuations seem to be slower than the μSR time window.

ZF- μSR experiments detected no additional static field below T_S . NMR spectral analyses are consistent with this observation. These results prove unambiguously that the ground state is not static magnetic order. This is in good contrast to the AF state in GeV_4S_8 established due to inter-cluster interactions.¹¹ As seen in Fig. 3, ^{71}K drops rapidly below T_S , which is well fit by $\exp(-E_g/k_B T)$ with the spin excitation gap $E_g/k_B \approx 220$ K. The Arrhenius plot of $^{71}(1/T_1)$, presented in Fig. 5(c), shows a good linearity in a wide T range well below T_S , and gives $E_g/k_B \approx 190$ K as the smallest gap, which is nearly the same as the spin gap estimated from ^{71}K . Hence, we conclude that the ground state of GaNb_4S_8 is a $S=0$ spin-singlet state. The T and field dependences of $\mu\text{SR}-\lambda$ also support this conclusion.

Characteristic precursory phenomena of the transition are summarized as (i) at the Nb site, the isotropic term of the

local susceptibility χ_{loc} looks suppressed from $\sim 3T_S$, and instead, large anisotropy appears, and (ii) around the Ga site, in contrast to moderate magnetic fluctuations, both static and dynamic structural fluctuations are enhanced from $\sim 3T_S$. As shown in Fig. 1, spin density distributions of HOMO are expected to be highly symmetric and asymmetric in the high- T and low- T states, respectively [similar discussions have been made on a $3d$ analog GaV_4S_8 (Refs. 12 and 13)]. On this basis, the above results are interpreted as follows; intracluster reconfiguration of Nb- $4d$ cluster orbitals (i.e., mixing of the low- T electronic state) already starts from $\sim 3T_S$, enhances intercluster structural instability, and finally induces cooperative long-range symmetry lowering at T_S , which is coupled with the spin degree of freedom.

As the mechanism of the spin-singlet formation, spin compensation via intercluster interactions should be considered, because each Nb_4 cluster unit has one unpaired electron with $S=1/2$. The crystallographically unique Nb_4 cluster even below T_S (Ref. 6) rules out charge disproportionation among clusters. According to the low- T lattice symmetry,⁶ all Nb_4 tetrahedra are elongated along one of the threefold axes $\langle 111 \rangle$ of the cubic lattice. As a result, two Nb_4 tetrahedra come closer slightly along the tetragonal $[110]$ or $[1\bar{1}0]$ direction. Hence, if electron-lattice coupling is appreciable, it is reasonable to expect binding of two Nb_4 tetramers to a Nb_8 octamer (Nb_4 - Nb_4 bond), just like the dimerization of the 1D spin chain. Considering this, the low- T upturn of χ may partly be due to unpaired clusters as defects. We speculate

that the transition at T_S is related with the characteristic electronic state of this material as a cluster Mott insulator,^{5,6,14} where the electron transfer is suppressed due to electron correlation, but is easily recovered by perturbation. Simultaneously, as mentioned above, we should note that this transition is driven by the local JT-type instability within the cluster. In this sense, the transition may be classified as the orbitally driven Peierls state,¹⁵ although intercluster spin-singlet correlation may also be developed from high- T of the order of spin gap. As a whole, the spin singlet state of GaNb_4S_8 is classified as one of exotic states found in frustrated lattices near metal-insulator boundaries; the crystal structure of GaNb_4S_8 is closely related to the highly frustrated pyrochlore lattice, and simultaneously Nb_4 units arrange as a frustrated fcc lattice.

In conclusion, μSR and NMR experiments revealed that the ground state of GaNb_4S_8 is a nonmagnetic spin singlet with an excitation gap of ~ 200 K. Taking into account the lattice symmetry below T_S , formation of a Nb_8 octamer from two Nb_4 tetramers is suggested for the first time. The transition is driven by the intracluster JT-type instability developed from high T of the order of $3T_S$.

This study was supported by Grant-in-Aid for Scientific Research on Priority Areas “Novel States of Matter Induced by Frustration,” (Grant No. 19052003), and Grant-in-Aid for Young Scientists (Start-up) (Grant No. 16076210) from MEXT, Japan.

¹R. E. Peierls, *Quantum Theory of Solids* (Clarendon Press, London, 1955).

²D. Brasen, J. M. Vandenberg, M. Robbins, R. H. Willens, W. A. Reed, R. C. Sherwood, and X. J. Pinder, *J. Solid State Chem.* **13**, 298 (1975).

³H. Ben Yaich, J. C. Jegaden, M. Potel, M. Sergent, A. K. Rastogi, and R. Tournier, *J. Less-Common Met.* **102**, 9 (1984).

⁴D. Johrendt, *Z. Anorg. Allg. Chem.* **624**, 952 (1998).

⁵R. Pocha, D. Johrendt, B. Ni, and M. M. Abd-Elmeguid, *J. Am. Chem. Soc.* **127**, 8732 (2005).

⁶S. Jakob, H. Müller, D. Johrendt, S. Altmannshofer, W. Scherer, S. Rayaprol, and R. Pöttgen, *J. Mater. Chem.* **17**, 3833 (2007).

⁷For example, W. Higemoto, H. Tanaka, I. Watanabe, and K. Nagamine, *Phys. Lett. A* **243**, 80 (1998); N. Cavadini, D. Andreica, F. N. Gyax, A. Schenck, K. Kramer, H.-U. Gudel, H. Mutka, and A. Wildes, *Physica B* **335**, 37 (2003).

⁸ K - χ plots at high T give the spin part in hyperfine coupling $^{93}\text{A}=-18.4$ and $^{71}\text{A}=0.089$ T/ μ_B , where we assumed the mo-

ment at each Nb atom and at each Nb_4 cluster for the cases of ^{93}Nb and ^{71}Ga , respectively.

⁹The values estimated from peak positions correspond to the component perpendicular to the principal axis, K_{\perp} . Therefore the isotropic shift K_{iso} is expected to deviate more strongly from the Curie-Weiss behavior.

¹⁰Below T_S , the Ga center line shows anisotropic broadening; the shift at the peak position corresponds to K_{\perp} . Note that the T dependence of $^{71}\text{K}_{\perp}$ below T_S , shown in Fig. 3, is stronger than that expected as K_{iso} .

¹¹H. Müller, W. Kockelmann, and D. Johrendt, *Chem. Mater.* **18**, 2174 (2006).

¹²R. Pocha, D. Johrendt, and R. Pöttgen, *Chem. Mater.* **12**, 2882 (2000).

¹³H. Nakamura, H. Chudo, and M. Shiga, *J. Phys.: Condens. Matter* **17**, 6015 (2005).

¹⁴M. Sieberer, S. Turnovszky, J. Redinger, and P. Mohn, *Phys. Rev. B* **76**, 214106 (2007).

¹⁵D. I. Khomskii and T. Mizokawa, *Phys. Rev. Lett.* **94**, 156402 (2005).